Internal Kink Instability during Off-Axis Electron Cyclotron Current Drive in the DIII-D Tokamak

K. L. Wong,[1] M. S. Chu,[2] T. C. Luce,[2] C. C. Petty,[2] P. A. Politzer,[2] R. Prater,[2] L. Chen,[3] R. W. Harvey,[4] M. E. Austin,[5] L. C. Johnson,[1] R. J. La Haye,[2] and R. T. Snider[2]

[1]*Plasma Physics Laboratory, Princeton University, Princeton, New Jersey 08543*
[2]*General Atomics, P.O. Box 85608, San Diego, California 92186*
[3]*Department of Physics, University of California, Irvine, California 92717*
[4]*CompX, Del Mar, California 92014*
[5]*University of Texas, Austin, Texas 78712*
(Received 5 November 1999)

Experimental evidence is reported of an internal kink instability driven by a new mechanism: barely trapped suprathermal electrons produced by off-axis electron cyclotron heating on the DIII-D tokamak. It occurs in plasmas with an evolving safety factor profile $q(r)$ when $q_{\min}$ approaches 1. This instability is most active when ECCD is applied on the high field side of the flux surface. It has a bursting behavior with poloidal/toroidal mode number $= m/n = 1/1$. In positive magnetic shear plasmas, this mode becomes the fishbone instability. This observation can be qualitatively explained by the drift reversal of the barely trapped suprathermal electrons.

PACS numbers: 52.35.Py, 52.35.Hr, 52.50.Gj, 52.55.Fa

The goal of the advanced tokamak program [1] is to produce and sustain a tokamak plasma with high confinement and high pressure over an extended period of time with well aligned bootstrap current. Off-axis electron cyclotron current drive (ECCD) in negative central shear (NCS) plasmas is a viable path towards this goal. The first experiments on off-axis ECCD have been successfully carried out on the DIII-D tokamak recently [2]. In these experiments, strong MHD activities were observed when the second harmonic cyclotron resonance layer was placed on the high magnetic field side of the flux surface just outside $q = 1$. In this paper, we present these data with an interpretation based on resonant wave-particle interaction.

It is well known that electron cyclotron waves can modify MHD activities in tokamaks. Suppression of the $m/n = 2/1$ mode using electron cyclotron heating (ECH) was demonstrated in TFR [3], JFT-2M [4], and TEXT [5]. Modification of sawtooth activities was observed in T-10 [6], DIII-D [7], and TCA [8], and control of neoclassical tearing mode by ECCD was demonstrated recently in ASDEX Upgrade [9]. In these experiments, MHD activities were modified through changes of plasma pressure, resistivity, and/or current density profile. The changes in MHD behavior reported here are believed to be due to resonant interaction with suprathermal electrons: a mechanism which has not been identified before. While energetic ions are found to drive MHD instabilities like fishbones [10] and Alfvén eigenmodes [11], similar interaction with energetic electrons is also possible when certain criteria are met. The result presented here is the first attempt to address this issue in ECCD/ECH experiments.

Fishbone instabilities in tokamaks are $m = 1$ internal kink modes driven by deeply trapped energetic ions via precessional resonance [12]. It was first observed in the PDX tokamak during perpendicular neutral beam injection; later experiments show that perpendicular injection is not necessary. The energetic ion pressure gradient is the source of free energy for this instability. The beam deposition profile peaks near the magnetic axis and the mode propagates poloidally parallel to the ion diamagnetic drift velocity ($k_\theta \parallel v_{\mathrm{di}}$) and toroidally parallel to the precession velocity $\langle v_\phi \rangle$ of deeply trapped ions which is in the same direction as the plasma current. Since effective energy exchange during wave-particle interaction requires that the particles resonate with the wave, one would not expect electrons and ions to resonate with the same mode and drive it together because they usually drift in opposite directions due to their opposite electric charges.

During off-axis ECCD experiments, a small number of suprathermal electrons are preferentially heated by obliquely propagating waves [13]. In our analysis, the bulk of the electron distribution function $f(v)$ is represented by a Maxwellian $f_m(v)$, and the suprathermal electrons are those in the tail of $f(v)$ which deviates from $f_m(v)$. We use the TORAY ray tracing code to calculate the wave absorption profile and the CQL3D Fokker-Planck code to calculate the bounce-averaged electron distribution function. Detailed analysis was carried out for shot 96163 where the resonance layer was placed at the high field side of the flux surface. The calculated wave power deposition peaks near $\rho = r/a = 0.16$, and so does the suprathermal electron energy density as depicted in Fig. 1(a). On this flux surface, calculations show that 1.4% of the electrons are suprathermal electrons with 7.9% of the total electron energy; 0.27% electrons have energy above 36 keV, and they possess 3.4% of the electron energy. The calculated population of barely trapped electrons with energy above 36 keV has hollow profiles as shown in Fig. 1(b). Therefore, in the region where the energetic trapped electron density gradient is

 0031-9007/00/85(5)/996(4)$15.00

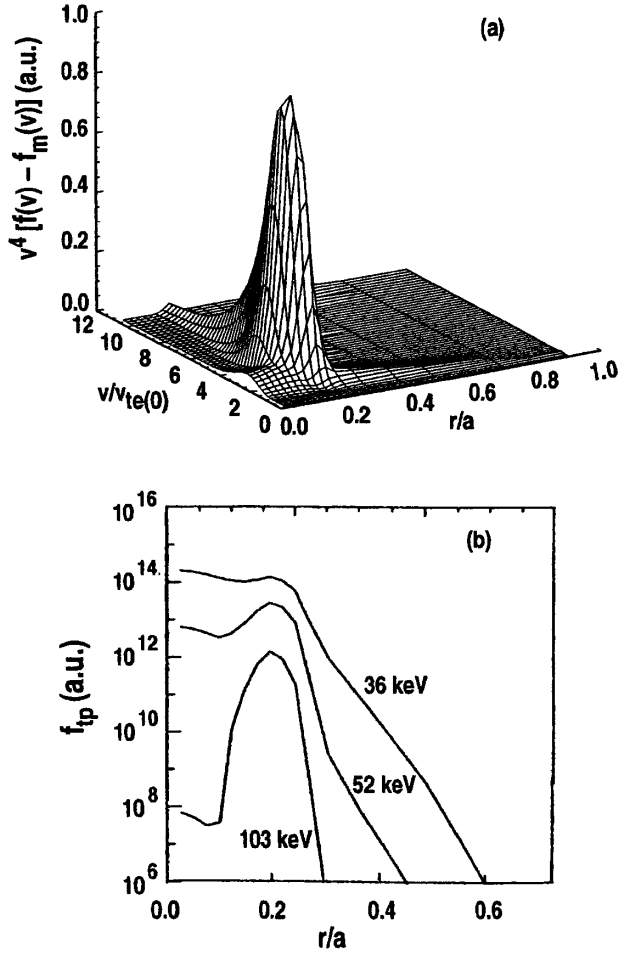

FIG. 1. Calculated suprathermal electron distribution in shot 96163. (a) Velocity spectrum of suprathermal electron energy versus radius. (b) Spatial profile of f_{tp}—the distribution function for electrons at the trapped-passing boundary with specified energies. Cross field transport is neglected in the calculation.

positive, the diamagnetic drift velocity of these electrons is parallel to that of the energetic ions produced by neutral beam injection. The precessional direction of the trapped electrons on the outboard side (at poloidal location $\theta < 90°$) is opposite to that of the deeply trapped ions; it reverses direction [14] at $\theta > 90°$ because the vertical component of the poloidal magnetic field reverses sign. For barely trapped electrons, the precessional direction averaged over the entire orbit is parallel to that of the deeply trapped ions because these electrons spend more time on the inboard ($\theta > 90°$) side so that this part of the orbit is weighted more heavily. Because of this drift-reversal effect, the barely trapped suprathermal electrons in the same energy range as the fast ions from neutral beam injection can resonate with fishbone modes. The hollow pressure profile of these electrons provides the free energy from the electron channel to assist the drive. Since the $m = 1$ internal kink modes are the most common precursor of sawtooth events, they are usually near marginal stability just prior to sawtooth activities, and this is the time that the electron drive is most likely to be noticeable. In this paper, we present experimental evidence indicating that this is occurring in the DIII-D ECCD experiment.

The experiment was carried out in the DIII-D tokamak with the following parameters: $B_T = -1.77$ T, $I_p = 0.89$ MA, $R = 1.76$ m, $a = 0.62$ m, $q_{95} = 6.06$, $q_{\min} \sim 1$, $\rho_{\min} \sim 0.2$ which is near the flux surface where peak wave power absorption occurs. Figure 2(a) is the schematic which shows the magnetic surfaces, the vacuum ray trajectories of the injected 110 GHz microwave power, and the location of the second and the third harmonic cyclotron resonance layers. The wave absorption occurs near the second harmonic resonance layer ($\omega = 2\omega_{ce}$) which is on the high field side of the magnetic surface. The electron temperature profile in the plasma core is measured from electron cyclotron emission (ECE) at the second harmonic frequency. The ECE radiometer is a 32 channel system and the channel locations are represented by the diamonds on the midplane depicted in Fig. 2(a). The electron temperatures measured by ECE are in good agreement with measurements from Thomson scattering.

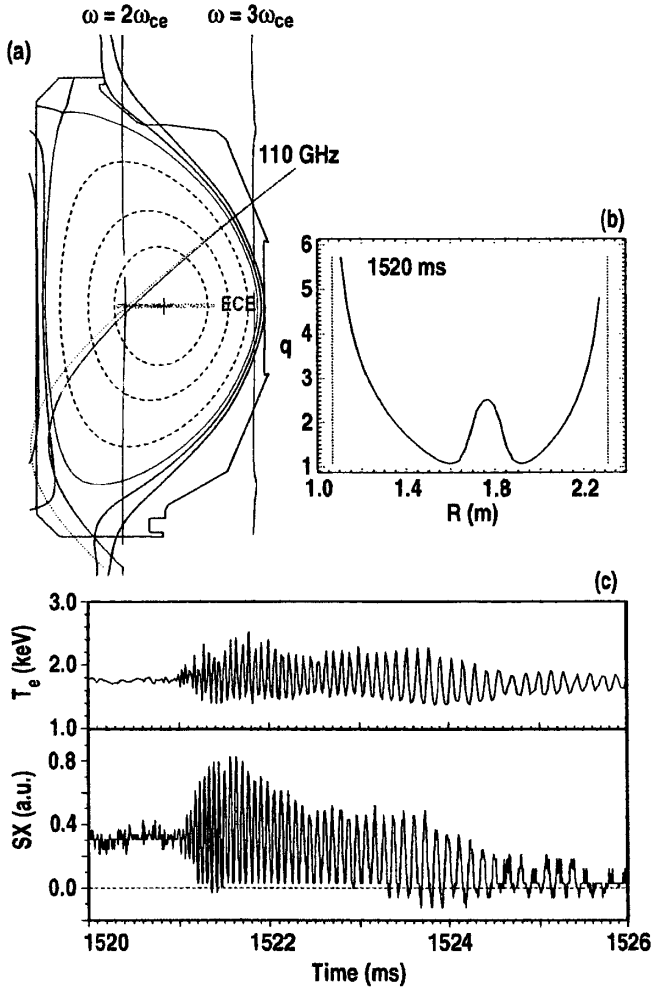

FIG. 2. (a) Schematic of the experimental setup. (b) Safety factor $q(r)$ at $t = 1.52$ s. (c) MHD oscillations near 1.52 s with varying frequency detected by ECE and soft-x-ray emission.

The 2.5 MW of deuterium neutral beam from a single source is injected into DIII-D starting at $t = 0.5$ s during the current ramp to produce the NCS plasma. The 1.1 MW of 110 GHz microwave power from two gyrotrons is injected at $t = 1.2$ s. One gyrotron is turned off at $t = 2.2$ s, and the other one at 2.4 s. At $t = 1.52$ s, the plasma q profile has strong NCS with $q(0) = 2.6$, $q_{\min} \sim 1.0$ [Fig. 2(b)], and bursts of MHD activities start to appear in ECE, soft-x-ray, and Mirnov loop signals. In most of the cases, the frequency is fixed at a value near 10 kHz which is close to the toroidal rotation frequency at the $q = 1$ surface measured by charge-exchange recombination spectroscopy. This is consistent with the toroidal mode number $n = 1$ determined by the toroidal array of Mirnov loops. Sometimes the frequency droops as shown in Fig. 2(c), and sometimes it remains constant. The cause of different behavior is not understood.

When the mode frequency changes with time, it is difficult to determine the poloidal mode number from Mirnov coil data. We analyze the ECE data with the singular-value-decomposition (SVD) technique [15]. The deviation of the electron temperature from the average temperature, δT_e, is analyzed. Figures 3(a) and 3(b) show the results for the time interval $t = 1.5$–1.6 s when there is 1.1 MW of ECH power. The topos (spatial eigenfunction) clearly shows a $m = 1$ structure (m is the poloidal mode number). The chronos (temporal eigenfunction) exhibits the growth and decay of the mode. Each burst correlates with a drop in the central electron temperature as detected by ECE measurements shown in Fig. 3(c). These are $m/n = 1/1$ modes. Stability analysis by the GATO code [16] (which does not treat energetic particles) shows that the $1/1$ mode is stable for this plasma equilibrium. The existence of the $1/1$ mode suggests the presence of energetic particle (ions and electrons) drive. There is an intrinsic uncertainty of order 0.1 in the motional Stark effect measurement of $q(r)$. Should $q_{\min}$ fall below 1.0, these would be double kink modes [17].

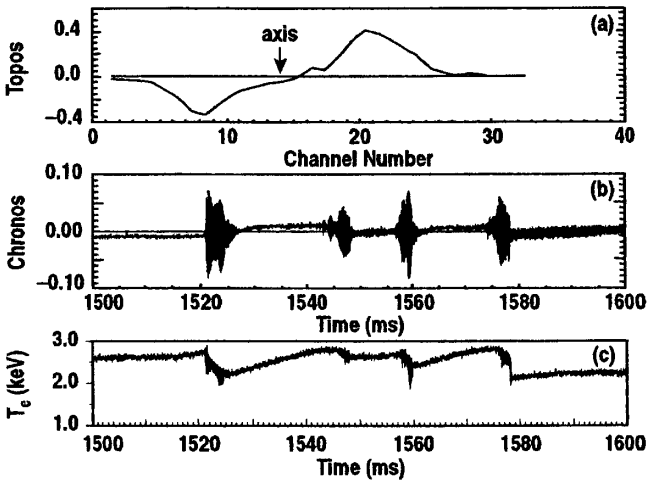

FIG. 3. Results from SVD analysis of ECE data from 1.5–1.6 s. (a) Topos showing $m = 1$ structure. (b) Chronos of the $m = 1$ mode showing the bursting behavior. (c) Dips in central electron temperature (ECE that correlates with the MHD burst).

The plasma q profile evolves with time during the shot. After $t = 1.72$ s, $q(0)$ drops to a value near $q_{\min}$ which is close to 1.0, and MHD bursts can appear between sawtooth crashes. A burst at $t = 1.82$ s is chosen for detailed analysis when $q(r)$ is flat in the plasma core. The plasma equilibrium is analyzed with the EFIT code [18], and the results are used by the GATO code for stability analysis. The $1/1$ mode is marginally unstable in this case and the mode structure is obtained. From the plasma displacement ξ on the midplane, we calculate the topos by $\delta \mathbf{T}_e = \xi d\mathbf{T}_e/dr$. The result is in reasonable agreement with experimental observations. Near the end of the ECH pulse, one gyrotron is turned off 200 ms before the other. It is found that during the high power phase, the instability grows faster, and most of them end abruptly in a crash event occurring much shorter than the growth rate.

Let θ_{res} denote the poloidal angle coordinate of the electron cyclotron wave absorption peak. The data presented so far come from the shot with $\theta_{\text{res}} \sim \pi$ (shot 96163). This is the shot in which the $m = 1$ internal kink instability is most active and the sawtooth activities appear earliest in time. By variation of the microwave injection angle and small changes in the magnetic field, θ_{res} is varied from π to $\pi/2$ in the experiment, and it is found that the instability becomes progressively weaker and the sawtooth activities appear later in the discharge. This trend is true not only for NCS target plasmas, it is also true for plasmas with positive central shear as depicted in Fig. 4, which shows that the number of $1/1$ bursts which appear before the first sawtooth crash increases with θ_{res}. The q profiles for these shots at the time of interest are quite similar; they all have positive central shear with $q_{\min} = q(0) \sim 1.0$. However, no two plasma shots are identical; there are minor differences in $q(r)$ as well as in other plasma parameters. In order to establish the effect of suprathermal electrons, we have to rule out the effect from the energetic ions whose population is proportional to $S_n/\langle n_e \rangle$—the neutron emission rate divided by the plasma density. By comparing shots with different $1/1$ activities and θ_{res}, we found 14 pair of shots where in each pair, the shot with stronger $1/1$ activity has an equal or slightly smaller value of $S_n/\langle n_e \rangle$, indicating that the difference in the $1/1$ activity is not due to the energetic ions. A clear trend emerges from this ensemble: the shot with stronger $1/1$ activity always has larger θ_{res}. This is a strong indication that barely trapped suprathermal electrons take part in driving the $1/1$ mode. $S_n/\langle n_e \rangle$ is about the same in the top three panels of Fig. 4; it is 25% higher in the bottom panel, and the similarity between this figure and Fig. 1 of Ref. [10] becomes easy to understand: they are the same fishbone modes with different driving mechanisms. The modes observed in PDX are driven purely by deeply trapped energetic ions while the excitation of the modes shown in Fig. 4(d) here is aided by barely trapped suprathermal electrons. They appear just before the sawtooth crash when the $m = 1$ internal kink is

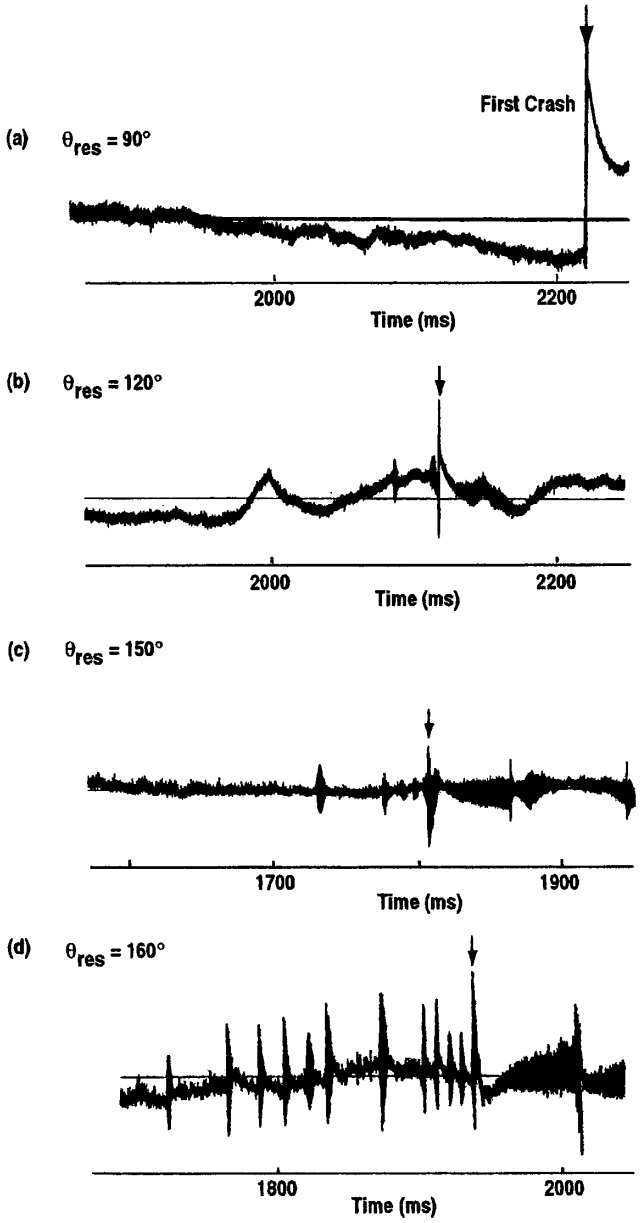

FIG. 4. Results from SVD analysis of ECE data showing variation of the $m/n = 1/1$ internal kink activity with the poloidal location of the second harmonic electron cyclotron resonance. Only one gyrotron is used in this sequence of shots.

near marginal stability. Instabilities excited by two energetic particle species have been observed in the past [19]. The data presented here were obtained from ECCD experiments with obliquely launched electron cyclotron waves. If the instability is excited by the trapped electrons rather than the wave-driven current, similar instability will be excited by perpendicularly launched waves which heat electrons with negligible driven current. Such an experiment was carried out recently. Indeed, the same instability was excited by electron heating at $\theta_{\rm res} \sim 180°$. This is additional evidence for the new instability mechanism.

In summary, we have shown that the behavior of internal kink modes in off-axis ECCD experiments in DIII-D can be explained by the wave-particle interaction with suprathermal electrons. The results presented here can also be viewed as an indirect evidence of drift reversal of barely trapped particles in a tokamak. This instability may impose some constraint on ECCD experiments, but it is not a serious obstacle because the energetic electron pressure gradient is highly localized in space. A small radial shift in the heating location (by a few centimeters) from the $q = 1$ surface will diminish the hot electron drive. The energetic fraction will be small in high density plasmas. This instability requires the presence of the $q = 1$ surface in the plasma. The target plasma for the advanced tokamak program on DIII-D has $q_{\rm min} > 1$, and therefore this instability is avoided.

We thank the DIII-D technical staff for their contribution to this experiment, and Dr. Vincent Chan for very helpful discussions. This work is supported by the United States Department of Energy under Contracts No. DE-AC02-76CH03073, No. DE-AC03-99ER54463, and Grant No. DE-FG03-97ER54415.

[1] A. D. Turnbull *et al.,* Phys. Rev. Lett. **74**, 718 (1995).
[2] T. C. Luce *et al.,* Phys. Rev. Lett. **83**, 4550 (1999).
[3] TFR Group FOM ECRH Team, Nucl. Fusion **28**, 1995 (1988).
[4] K. Hoshino *et al.,* Phys. Rev. Lett. **69**, 2208 (1992).
[5] D. C. Sing *et al.,* Phys. Fluids B **5**, 3239 (1993).
[6] G. A. Bobrovskii, Yu. V. Esipchuk, and P. V. Savrukin, Sov. J. Plasma Phys. **13**, 665 (1987).
[7] R. T. Snider *et al.,* Phys. Fluids B **1**, 404 (1989).
[8] Z. A. Pietrzyk *et al.,* Nucl. Fusion **33**, 197 (1993).
[9] H. Zohm *et al.,* in *Proceedings of the 25th EPS Conference on Controlled Fusion and Plasma Physics, Prague, Czech Republic, 1998* (European Physical Society, Petit-Lancy, 1998), p. 480.
[10] K. McGuire *et al.,* Phys. Rev. Lett. **50**, 891 (1983).
[11] K. L. Wong, Plasma Phys. Controlled Fusion **41**, R1 (1999).
[12] Liu Chen, R. B. White, and M. N. Rosenbluth, Phys. Rev. Lett. **52**, 1122 (1984).
[13] V. Erckmann and U. Gasparino, Plasma Phys. Controlled Fusion **36**, 1869 (1994); also C. F. F. Karney and N. J. Fisch, Nucl. Fusion **21**, 1549 (1981).
[14] B. B. Kadomtsev and O. P. Pogutse, Nucl. Fusion **11**, 67 (1971).
[15] T. Dudok de Wit, A.-L. Pecquet, J.-C. Vallet, and R. Lima, Phys. Plasmas **1**, 3288 (1994).
[16] L. C. Bernard *et al.,* Comput. Phys. Commun. **24**, 377 (1981).
[17] L. L. Lao *et al.,* Nucl. Fusion **30**, 1035 (1990).
[18] J. W. Connor *et al.,* in *Proceedings of the 16th IAEA Fusion Energy Conference, Montreal, 1996* (International Atomic Energy Agency, Vienna, 1997).
[19] K. L. Wong *et al.,* Phys. Rev. Lett. **76**, 2286 (1996).